Electronic properties of antidot lattices fabricated by atomic force lithography

A. Dorn, M. Sigrist, A. Fuhrer, T. Ihn, T. Heinzel, and K. Ensslin[a)]
Solid State Physics Laboratory, ETH Zürich, 8093 Zürich, Switzerland

W. Wegscheider
Angewandte und Experimentelle Physik, Universität Regensburg, 93040 Regensburg, Germany

M. Bichler
Walter Schottky Institut, TU München, 85748 Garching, Germany

(Received 19 June 2001; accepted for publication 14 November 2001)

Antidot lattices were fabricated by atomic force lithography using local oxidation. High quality finite 20×20 lattices are demonstrated with periods of 300 nm. The low-temperature magnetoresistance shows well developed commensurability oscillations as well as a quenching of the Hall effect around zero magnetic field. In addition, we find B-periodic oscillations superimposed on the classical commensurability peaks at temperatures as high as 1.7 K. These observations indicate the high electronic quality of our samples. © *2002 American Institute of Physics.* [DOI: 10.1063/1.1432767]

Experiments on lateral superlattices have revealed a variety of unexpected phenomena in the classical as well as in the quantum regime. Antidot lattices are particularly appealing for studying how a classically chaotic system develops quantum signatures for shorter lattice periods.[1–6] Most high-quality samples have so far been fabricated with electron beam lithography. This technology is well developed and offers reliable performance as well as excellent electronic quality of the fabricated samples down to lattice periods of about 100 nm.[7,8] The quest for the experimental observation of a quantum mechanical band structure based on the periodic lateral potential modulation is ongoing and requires lattice periods of the order of the Fermi wavelength of the electrons in the two-dimensional electron gas (2DEG). Lattice periods of the order of 40–50 nm are difficult to fabricate by electron beam lithography due to the proximity effect.

Lithography based on scanning probe techniques has evolved into a powerful tool for defining ultrasmall patterns on surfaces.[9] Electronically functional lateral superlattices have been fabricated by using the (sharpened) tip of an atomic force microscope (AFM) to either scratch a pattern in a resist layer[10] or directly scratch into the surface of an InAs heterostructure.[11] An alternative approach relies on the local oxidation of a water covered surface by applying a voltage between a conductive AFM tip and the underlying surface.[12] If applied to AlGaAs heterostructures a two-dimensional electron gas close enough to the sample surface (less than 50 nm for practical considerations) has been shown to be depleted below the oxidized lines.[13] This procedure has the desirable property that the pattern transfer occurs simultaneously with the lithography step and no further treatment/processing is needed. It has been demonstrated that electronically tunable quantum wires[14] and quantum dots[15] can be fabricated with this technology. Important features of nanostructures fabricated this way are the smooth[16] as well as steep[17] potential walls. These are crucial ingredients for the successful realization of lateral superlattices.

We started from a high-quality two-dimensional electron gas with a 4 K mobility of $\mu=800'000\ \mathrm{cm^2/V\,s}$ and an electron density of $N_s=5\times10^{11}\ \mathrm{cm^{-2}}$. The electron gas embedded in the AlGaAs heterostructure was 34 nm below the sample surface. For lithography we used a commercial Digital Instruments Dimension 3100 with metrology head. This AFM is equipped with capacitive sensors that reduce long time drifts and creep through a hardware feedback and enable a lateral positioning of the tip with a precision in the nm range. The humidity of the atmosphere surrounding tip and sample is kept at a value of about 40% during the writing process. Typical voltages for the oxidation of the GaAs surface were -10 to -30 V applied to the tip with the GaAs grounded. The oxide pillars in this structure were written in tapping mode with a stationary 3 s/-18 V pulse at each site. The pillars show a high uniformity and have a cone-like shape with a base of about 250 nm and a height of about 8 nm.

For large antidot arrays we observed a weakening of the oxidation process either caused by a deterioration of the AFM tip and/or an insufficient supply of water on the surface as many oxide pillars are formed. In this letter we present results on a 20×20 array where we are safely within the limit of a uniform pattern.

After the AFM process the sample is covered with a uniform metallic layer which allows us to tune the Fermi energy of the lattice and in addition protects the sample surface from contamination or further oxidation.

It is well known that the piezos which drive the scanning unit have intrinsic creep and hysteresis properties. While the results of these unwanted features can be eliminated to some degree by software in the imaging mode, they can have detrimental consequences for lithography. As long as single nanostructures are envisioned, such as dots and wires, small

a)Electronic mail: ensslin@phys.ethz.ch

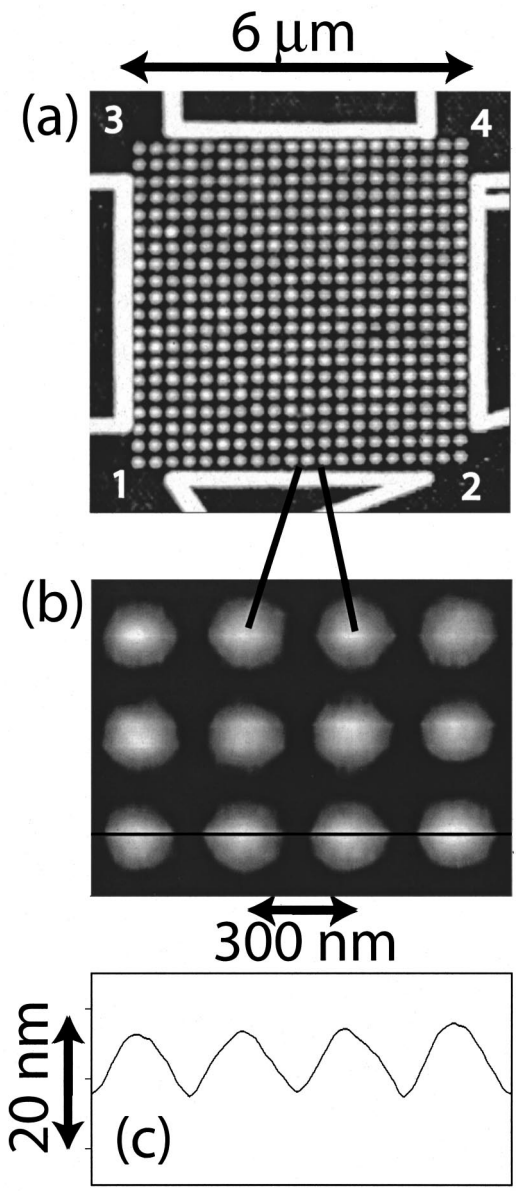

FIG. 1. (a) Overview of the entire AFM patterned area. The bright areas mark the oxidized regions below which the electron gas is depleted. The contacts are numbered 1–4. (b) Close-up of a 3×4 period segment from (a). (c) Line scan along the direction indicated in (b).

imperfections of their shape can be tolerated since the potential landscape has some random background due to the modulation doping anyway. For periodic lattices, however, creep and hysteresis can lead to errors of the order of the lattice period for arrays with periods below 100 nm. It is, therefore, crucial for the precision of our pattern that we have hardware control over the actual position of the AFM tip as described above.

Another limitation for the precision of periodic lattices fabricated by AFM lithography is thermal drift which cannot easily be compensated by hardware since it affects the entire instrument. We found empirically that a carefully controlled lab environment ($\Delta T<0.5$ K) in combination with settling times of the order of several hours reduce the thermal drift to values which are no longer detectable in our antidot lattices.

Figure 1(a) shows an overview of the entire 20×20 array with a lattice period of 300 nm. The bright areas are patterned with the AFM and define the regions of depleted

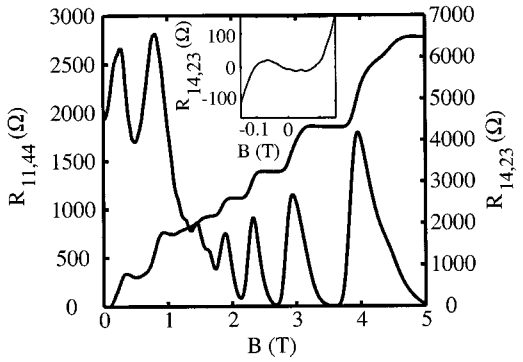

FIG. 2. Four-terminal magnetoresistance (left-hand scale) and Hall resistance (right-hand scale) at $T=1.7$ K through the finite antidot geometry; contacts are numbered as indicated in Fig. 1(a). The inset shows a close-up of the Hall effect around B=0.

electron gas. The four outer bars are necessary to define a measurement geometry for the finite lattice. Typical breakdown voltages between areas of 2DEG separated by insulating lines are $\geqslant1$ V at $T=4.2$ K. The close-up presented in Fig. 1(b) as well as the line scan in Fig. 1(c) show the precision obtained with this technology. From an analysis of the topography of the entire lattice we estimate the error in antidot position to be $\Delta a/a\approx1\%$, and the variation in antidot size to be less than 5%.

Figure 2 shows the magnetoresistance of the structure presented in Fig. 1 at $T=1.7$ K. The resistance $R_{11,44}$ is a two-terminal resistance with respect to the square geometry. However, there are two independent ohmic contacts in each of the corresponding electron gas regions next to the square geometry in order to eliminate contact resistances. The magnetoresistance measured this way displays the well known commensurability maxima which are related to classical cyclotron orbits around 1 ($B\approx0.8$ T) resp. 4 ($B\approx0.2$ T) antidots. At high magnetic fields where the cyclotron diameter becomes much smaller than any of the lattice features, Shubnikov–de Haas oscillations are recovered. The Hall resistance $R_{14,23}$ displays plateau-like features close to the commensurability conditions and a quenching around B=0. All of these features are well known from previous experiments.[2,6] The quality of the features as presented in Fig. 2 shows that the electronic potential landscape created by AFM lithography is at least comparable to those obtained by conventional electron beam lithography. From the shape of the classical maxima in the magnetoresistance as well as from the onset of Shubnikov–de Haas oscillations we estimate the electronic size of an antidot at the Fermi energy to be less than 200 nm. This is consistent with the lithographic size as well as with the lateral depletion length obtained for wires[14] and dots[17] fabricated with the same technology.

In addition to the classical effects, we observe fluctuations and oscillations of phase coherent origin superimposed on the main commensurability maximum. In order to resolve these effects most clearly, the carrier density is reduced by applying a negative gate voltage of $V_g=-100$ mV. Figure 3 shows $R_{11,44}$, where the point contacts still support several one-dimensional modes, but the antidots have become large enough at the Fermi surface, that the magnetoresistance maximum corresponding to a ballistic orbit around four antidots is eliminated. In this regime it has been demon-

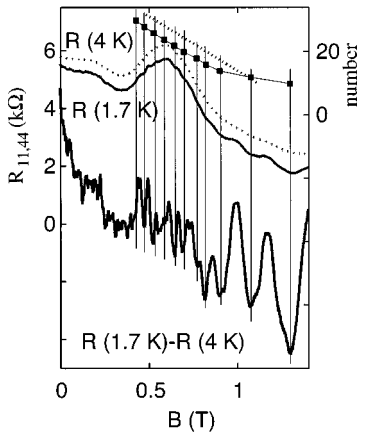

FIG. 3. Three curves showing the resistance at $T=4.2$ K (top curve, dashed line), at $T=1.7$ K (solid line, vertically offset by 0.5 kΩ), and the difference (bottom curve). Thin vertical lines connect minima in the magnetoresistance with the very top curve where the minima are plotted according to their number which is extrapolated from filling factors extracted from the high-field Shubnikov–de Haas oscillations. The straight dashed line shows the behavior expected for consecutively adding flux quanta through a circle with diameter 300 nm.

strated that B-periodic oscillations can be observed in an infinite lattice.[4] For a finite lattice much smaller than ours, on the other hand, these quantum oscillations are dominated by ballistic conductance fluctuations.[5] In our case where the phase coherence length is much larger than the lattice period but probably comparable or smaller than the extent of the finite lattice, we observe both types of phase coherent phenomena at $T=1.7$ K. In Fig. 3 we show $R_{11,44}$ at $T=4.2$ K (dashed line), at $T=1.7$ K (solid line, vertically offset by 0.5 kΩ) and the difference between these two curves (solid curve). Coming from high magnetic fields, Shubnikov–de Haas oscillations dominate the magnetoresistance. By numbering the minima with appropriate filling factors (the 2D density is $N_s=3.1\times10^{11}$ cm^{-2}) we continue this procedure down to magnetic fields $B\leqslant1$ T where the magnetoresistance minima no longer follow a 1/B periodicity. The corresponding positions are plotted in the upper part of Fig. 3. In the regime where the electrons classically encircle a single antidot, the orbits can no longer contract for increasing magnetic field, since the Lorentz force is increasingly compensated by electrostatic deflection off the antidot pillars. In this regime the magnetoresistance minima follow a B rather than a 1/B periodicity.[4,18,19] Because our lattice is finite, additional features occur in the magnetoresistance due to ballistic phase coherent fluctuations.[5]

We have demonstrated that high-quality antidot lattices can be fabricated by AFM-mediated local oxidation of AlGaAs heterostructures. The experimentally observed features, e.g., classical commensurability oscillations superimposed by phase coherent fluctuations, demonstrate that the electronic potential landscape can at least compete with the best samples prepared by other means. Since our technological approach is based on scanning probe techniques, it offers the intrinsic advantage to fabricate samples with substantially smaller lattice periods. This requires high-quality 2DEGs close to the sample surface. Furthermore, one of the major challenges is to keep the uniformity of the pattern for smaller periods and thinner oxide pillars.

The authors are grateful to the Swiss Science Foundation (Schweizerischer Nationalfonds) for financial support.

[1] K. Ensslin and P. M. Petroff, Phys. Rev. B **41**, 12307 (1990).
[2] D. Weiss, M. L. Roukes, A. Menschig, P. Grambow, K. v. Klitzing, and G. Weimann, Phys. Rev. Lett. **66**, 2790 (1991).
[3] A. Lorke, J. P. Kotthaus, and K. Ploog, Superlattices Microstruct. **9**, 103 (1991).
[4] D. Weiss, K. Richter, A. Menschig, R. Bergmann, H. Schweizer, K. v. Klitzing, and G. Weimann, Phys. Rev. Lett. **70**, 4118 (1993).
[5] R. Schuster, K. Ensslin, D. Wharam, S. Kühn, J. P. Kotthaus, G. Böhm, W. Klein, G. Tränkle, and G. Weimann, Phys. Rev. B **49**, 8510 (1994).
[6] For a review, see R. Schuster and K. Ensslin, Adv. Solid State Phys. **34**, 195 (1994).
[7] T. Schlösser, K. Ensslin, J. P. Kotthaus, and M. Holland, Europhys. Lett. **33**, 683 (1996).
[8] C. Albrecht, J. H. Smet, K. von Klitzing, D. Weiss, V. Umansky, and H. Schweizer, Phys. Rev. Lett. **86**, 147 (2001).
[9] For a review, see *Technology of Proximal Probe Lithography*, edited by C. R. K. Marrian (SPIE Optical Engineering, Bellingham, WA, 1993).
[10] M. Wendel, H. Lorenz, and J. P. Kotthaus, Appl. Phys. Lett. **67**, 3732 (1995).
[11] J. Cortes Rosa, M. Wendel, H. Lorenz, J. P. Kotthaus, M. Thomas, and H. Kroemer, Appl. Phys. Lett. **73**, 2684 (1998).
[12] R. S. Becker, J. A. Golavchenko, and B. S. Swartzentruber, Nature (London) **325**, 419 (1987); J. A. Dagata, J. Schneir, H. H. Harary, and C. J. Evans, Appl. Phys. Lett. **56**, 2001 (1990); H. Sugimura, T. Uchida, N. Kitamura, and H. Masuhara, *ibid.* **63**, 1288 (1993); D. Wang, L. Tsau, and K. L. Wang, *ibid.* **67**, 1295 (1995); E. S. Snow, D. Park, and P. M. Campbell, *ibid.* **69**, 269 (1996); E. S. Snow and P. M. Campbell, *ibid.* **64**, 1932 (1994); E. S. Snow and P. M. Campbell, Science **270**, 1639 (1995); E. S. Snow and P. J. McMarr, Appl. Phys. Lett. **66**, 1388 (1995); R. Held, T. Heinzel, P. Studerus, K. Ensslin, and M. Holland, *ibid.* **71**, 2689 (1997).
[13] R. Held, T. Vancura, T. Heinzel, K. Ensslin, M. Holland, and W. Wegscheider, Appl. Phys. Lett. **73**, 262 (1998).
[14] R. Held, S. Lüscher, T. Heinzel, K. Ensslin, and W. Wegscheider, Appl. Phys. Lett. **75**, 1134 (1999).
[15] S. Lüscher, A. Fuhrer, R. Held, T. Heinzel, K. Ensslin, and W. Wegscheider, Appl. Phys. Lett. **75**, 2452 (1999).
[16] T. Heinzel, G. Salis, S. Lüscher, R. Held, K. Ensslin, and W. Wegscheider, Phys. Rev. B **61**, R13353 (2000).
[17] A. Fuhrer, S. Lüscher, T. Heinzel, K. Ensslin, W. Wegscheider, and M. Bichler, Phys. Rev. B **63**, 125309 (2001).
[18] K. Richter, Europhys. Lett. **29**, 7 (1995).
[19] G. Hackenbroich and F. von Oppen, Europhys. Lett. **29**, 151 (1995).